

New microfluidic paper-based analytical device for iron determination in urine samples

Francisca T. S. M. Ferreira, Karina A. Catalão, Raquel B. R. Mesquita*, António O. S. S.
Rangel

*Universidade Católica Portuguesa, CBQF - Centro de Biotecnologia e Química Fina – Laboratório
Associado, Escola Superior de Biotecnologia, Rua Diogo Botelho 1327,
4169-005, Porto, Portugal*

*corresponding author: rmesquita@ucp.pt

Francisca T. S. M. Ferreira ORCID: 0000-0002-3921-3973

Raquel B. R. Mesquita ORCID: 0000-0001-7745-1860

António O. S. S. Rangel ORCID: 0000-0002-6486-8947

Abstract

Iron is an important micronutrient involved in several mechanisms in the human body and can be an important biomarker. In this work, a simple and disposable microfluidic paper-based analytical device (μ PAD) was developed for the quantification of iron in urine samples. The detection was based on the colorimetric reaction between iron(II) and bathophenanthroline and the reduction of iron(III) to iron(II) with hydroxylamine. The developed μ PAD enabled iron determination in the range 0.07 – 1.2 mg/L, with a limit of detection of 20 μ g/L and a limit of quantification of 65 μ g/L, thus suitable for the expected values in human urine. Additionally, targeting urine samples, the potential interference of the samples color was overcome by incorporating a sample blank assessment for absorbance subtraction. Stability studies revealed that the device was stable for 15 days prior to usage and that the formed colored product was stable for scanning up to 3 hours. The accuracy of the developed device was established by analyzing urine samples (#26) with the developed μ PAD and with the atomic absorption spectrometry method; the relative deviation between the two sets of results was below 9.5%.

Keywords: paper sensor, biological samples, bathophenanthroline reaction, sample blank correction, iron(II) and iron(III) content, disposable device

Declarations

Funding

This work was supported by National Funds from FCT through project UIDB/50016/2020. F.T.S.M. Ferreira thanks FCT - Fundação para a Ciência e a Tecnologia for the grant SFRH/BD/144962/2019.

Conflicts of interest/Competing interests

The authors declare that they have no conflict of interest.

Availability of data and material

Not applicable

Code availability

Not applicable

Authors' contributions

Conceptualization - Raquel B. R. Mesquita; Methodology - Francisca T. S. M. Ferreira, Karina A. Catalão; Validation - Francisca T. S. M. Ferreira; Formal analysis - Karina A. Catalão, Francisca T. S. M. Ferreira; Investigation - Karina A. Catalão, Francisca T. S. M. Ferreira; Resources - António O. S. S. Rangel; Writing - Original Draft Francisca T. S. M. Ferreira; Writing - Review & Editing - Raquel B. R. Mesquita, António O. S. S. Rangel; Project administration - Raquel B. R. Mesquita, António O. S. S. Rangel; Funding acquisition António O. S. S. Rangel

Ethics approval

The urine samples involved in this work were blind in-house samples, with no identification nor any information required or register, obtained from voluntary participants with informed consent. There was no association to a clinical trial.

Consent to participate

Not applicable.

Consent for publication

Not applicable

1. Introduction

Iron is one of the most studied micronutrients on Earth and it is crucial for the existence of life. This metal is associated to several important roles such as the transport, storage and use of oxygen, the correct function of hundreds of proteins and enzymes, the DNA synthesis, among others [1]. Because it is present in several biological mechanisms, iron metabolism is very tightly regulated and, both deficiency and overload of this metal can cause severe damages. The majority of the iron a human individual requires is achieved by recycling it from senescent blood cells, the remaining comes from diet intake [1, 2]. When it exceeds the normal concentration, the excretion occurs in urine [2]. The normal excretion rate is of approximately 100 $\mu\text{g}/\text{day}$ to 300 $\mu\text{g}/\text{day}$. In case of deficit or excess of the ingested iron, excretion will be less or more than normal, respectively [3]. A few common diseases associated with the deregulation of iron are anemia, hemochromatosis ($>20 \text{ mg}/\text{day}$), cancer and neurodegenerative diseases [1, 3]. Because of all the relevant roles and common diseases related to iron regulation in the human body, it is essential to have simple, rapid, and effective monitoring tool. Currently, urinary iron is mostly determined by inductively coupled plasma (ICP) combined with either mass or optical emission spectrometry; however, these techniques require costly and complex equipment [3–5]. According to the World Health Organization, even with the constant technology evolution, there is still a lack of practical and affordable devices and techniques that can perform diagnosis and treatments on location, particularly in the most secluded areas [6, 7].

Although the use of paper in analytical determinations dates back to the XVII century, the concept of microfluidic paper-based analytical devices (μPADs) was first reported by Martinez A. as a “platform for inexpensive, low-volume, portable bioassays” [8, 9]. There are two different areas that are characteristic of these devices, the hydrophilic and the hydrophobic area [8, 10]. The first provides the support for the reaction and is typically composed by paper, since it is low cost, has high availability, is lightweight and available in several thicknesses and porosities. Furthermore, paper is easy to store and transport and compatible with biological samples, because of its cellulose matrix [11]. The hydrophobic area limits the reaction area and can be achieved in numerous ways and composed by several materials. One of the most common approach is wax printing since it is a simple, and relatively fast method compatible with most μPAD applications,

however, this type of printing method requires expensive wax and an extra step of heating in the process [10, 12]. Nowadays there are several types of reactions reported to be used in μ PADs; however, the most common are the colorimetric reactions since the results can be simply interpreted visually or captured with any mobile device, from digital cameras to mobile phones or portable scanners [8, 12]. From there, absorbance values can be obtained from the color intensities measured by image processing [13]. The main disadvantage of the use of the colorimetric reactions in paper is the possible high variability caused by a non-uniform distribution of the colored product in the paper, however this problem can be reduced by using more replicates and excluding outliers, if necessary [8]. In recent years, the μ PADs popularity increased mainly due to their various advantages like being simple, portable, affordable, rapid, disposable, and after being assembled don't require complex equipment or specialized personal to do the measurement, which makes them an interesting tool to be used as on-site analysis in locations of difficult access or with very few resources [14]. However, very few of the developed μ PADs reported so far, presented any on-field or stability studies [8]. Because, some locations or conditions can affect the performance of these devices, it is very important to test them on lab conditions, on field conditions and also their stability in different storage conditions [7, 8]. In the human body, iron is present in two different oxidation states, the divalent ferrous (Fe^{2+}) and the trivalent ferric (Fe^{3+}), and it changes its state in order to participate in several biological reactions [15]. At the physiological pH, iron is usually present in the ferric state, Fe(III), although it is only absorbed as Fe(II) [16]. The determination of iron in biological fluids, namely urine, has then the potential of being useful for health diagnosis. However, although there are some reported works describing paper-based devices for iron determination [17–19], only the work by Kamlesh Shrivastava (2020) [19] targets the analyses of biological fluids (blood), in addition to water samples.

In this context, the aim of this work was to develop a new microfluidic paper-based analytical device (μ PAD) capable of performing on-hand quantification of iron in human urine samples, enabling to overcome potential sample color interference. Since iron can be present in both forms, an option was made to perform the determination of total iron. The assembly of the μ PAD relied in an innovative approach [20] and the detection was based on the colorimetric reaction of bathophenanthroline with iron(II) [21, 22], a

selective and sensitive methodology. To attain the determination of total iron, bathophenanthroline was combined with hydroxylamine, a well-known reducing agent capable of converting Fe (III) in Fe(II) [22]. To handle the potential color of the urine samples, sample intrinsic absorption, a sample blank approach was considered. As far as we know, it was the first time this approach was used in a paper-based platform. This feature was highly important to ensure the applicability of the developed μ PAD, as urine may present a wide variability of color range, from light yellow to brownish. In the end, this innovative solution, enabled the determination of total iron in several urine samples with the developed disposable device in an in-situ approach.

2. Materials and methods

2.1. Reagents and solutions

The solutions used in this work were prepared with analytical grade chemicals and deionized water (resistivity < 0.1 mS/cm).

A standard stock solution of 50 mg/L iron was monthly prepared by dilution of the iron atomic absorption standard solution (1000 mg/L) (Fluka, 16596-250 mL). The working standards were weekly prepared from the stock solution in the dynamic range of 0.1 – 1.2 mg/L Fe(III) in 5 mM of nitric acid.

A 1 g/L bathophenanthroline solution (BPS) was monthly prepared by dissolving 20 mg of bathophenanthroline disulfonic acid disodium salt hydrate (Alfa Aesar) in 20 mL of deionized water and stored in a dark bottle.

The hydroxylamine solution was prepared by dissolving 0.75 g of the solid (Sigma-Aldrich) in 7 mL of HCl 6 M and then completed to 50 mL with deionized water to final concentrations of 15 g/L hydroxylamine in 0.84 M of HCl. The 6 M HCl solution used was obtained from hydrochloric fuming acid (d = 1.19, 37%, Merck).

The working reagent solution (BPSH) was daily prepared by mixing 1 mL of BPS solution and 400 μ L of hydroxylamine solution and it was stored in a dark bottle and shielded from the light.

The synthetic urine used in the interference studies was prepared with the following concentrations: 10 g/L urea, 0.07 g/L uric acid, 0.8 g/L creatinine, 5.2 g/L sodium

chloride, 0.1 g/L lactic acid, 0.4 g/L citric acid, 0.37 g/L calcium chloride dihydrate, 0.49 g/L magnesium sulphate heptahydrate, 1.41 g/L sodium sulphate, 0.95 g/L potassium dihydrogen phosphate, 1.2 g/L potassium hydrogen phosphate and 0.49 g/L glucose, as reported by Machado [23].

2.2. Assembly of the μ PAD for iron determination and analytical procedure

The developed μ PAD (Fig. 1a) consisted in twenty filter paper units, as hydrophilic area, aligned in a 4 columns and 5 rows' distribution, inside of a laminating pouch (Q-Connect, 75x110 mm, glossy, 125 micron), as hydrophobic area (L1 and L2 – Fig. 1a). The paper units were placed under 5 mm holes, previously perforated using a puncher (KNIPEX), for the sample insertion (L1 – Fig. 1a). Each unit (Fig. 1b) consisted of two layers: top layer R1, the reagent layer, a paper disc Whatman Grade 1 filter, 9.5 mm diameter; and E1, an empty layer, a paper disc Whatman Grade 3 filter, 12,7 mm diameter. The reagent paper discs were prepared by adding 10 μ L of the working reagent solution (BPS_h) to the discs and then dried it in the oven for 15 min at 50 °C. After the alignment of the paper units with the sample insertion holes of the laminating pouch they were passed through the laminator (United Office – ULG 300 B1), where the plastic sheets of the pouch sealed around the paper units, creating a strong physical barrier between the units (Fig. 1c).

Figure 1 here, please

To perform the measurements, after assembly of the μ PAD, 40 μ L of sample/standard were inserted through the μ PAD sample hole. It was established to have 5 units for each standard/sample (corresponding to one column), to enable the exclusion of outliers (if necessary) and still have replicates. Once the sample/standard was completely absorbed, the sample holes were covered with adhesive tape, to prevent possible contaminations when handling the targeted biological samples.

The iron in the sample/standard reacts with the BPS and hydroxylamine mixture (BPS_h) while going through the reagent layer (layer R1) forming a pink color product. The intensity of pink color is directly proportional to the concentration of iron in the sample.

To measure the intensity of the color, the top layer of the μ PADs was scanned (Canon LiDE 120) and the images processed using an image software (ImageJ, National Institutes of Health, USA).

The time between the sample/standard introduction and the scanning of the μ PAD, named time-to-scan (TTS), was set to 20 minutes. In the ImageJ program, images were converted into RGB plots, and the green filter used to measure the intensity, since the expected colored product of the BPS reaction with iron is pink (from which the complementary color is green). For each unit, an option was made to do the measurements in the sample insertion hole where the colored product was concentrated (5 mm diameter) corresponding to a circular selection of 100×100 pixels, (Fig. 1d). The intensity values were then converted into absorbance values using the formula: $A = I_0/I_s$, where I_0 is the intensity of the blank signal, obtained when loading with deionized water, and I_s is the intensity of the standards/sample signal.

2.2.1. Urine sample μ PAD - the design adjusted to include sample blank

As the color measurement is based on a RGB filter selection (not a specific wavelength), the potential interference of the urine sample color was addressed. Urine has a highly variable color, intrinsic absorption, so the strategy for eliminating its potential interference consisted in incorporating, in the μ PAD card, the measurement of a sample blank. This measurement corresponded to the intensity values registered when loading the sample without the color reagent. For the absorbance calculation, a I_0 value is needed, so the sample μ PAD card also needed to include one column (with five units) for the corresponding blank signal, without BPS and to be loaded with water.

Therefore, only the reagent layer of the sample μ PAD was different from the reagent layer of the standards μ PAD (Fig. 1): two columns of the reagent layer included the color reagent (BPS) and other two columns just had hydroxylamine (Fig.2).

Figure 2 here, please

To analyze the urine sample, the two columns with BPS were prepared as mentioned above; one column (B1 in Fig. 2b) was loaded with 40 μ L of water, another one (S1 in Fig. 2b) loaded with 40 μ L of sample for total absorbance (A_T) calculation. As for the two

columns without BPS, the reagent layer (R1h) was prepared only with hydroxylamine solution (without the color reagent BPS) and aligned on top of the empty layer (E1). Again, one column was loaded with water and one column loaded with sample (B2 and S2, respectively, Fig. 2b); the calculated absorbance corresponded to the sample blank (A_{SB}).

The iron concentration of the sample was calculated based on the absorbance corresponded to the absorbance value resulting from the color reaction (A_{CR}): $A_{CR} = A_T - A_{SB}$

2.3. Samples

The urine samples were collected as “blind samples” from volunteers with their informed consent and stored at $-20\text{ }^{\circ}\text{C}$ until used. The samples that showed turbidity (suspended solids) were filtrated using disposable syringe filters with a pore size of $0.45\text{ }\mu\text{m}$ (Chromafil® Pet -45/25; polyester). All samples were acidified to 5 mM of nitric acid before being analyzed.

Human and Animal Rights

As the urine samples involved in this work were blind in-house samples obtained directly from informed voluntary participants and no identification nor any extra information required, all rights were respected.

2.4. Reference Procedure - Validation

To assess the accuracy of the developed μPAD for the iron determination in urine samples, a comparison was made between the results obtained with the μPAD and those obtained by atomic absorption spectrometry (AAS). For the AAS procedure, a calibration curve in the range $0.1 - 1.5\text{ mg/L}$ was established with iron(III) standards according to the reference protocol [24]. The urine samples were prepared as described in section 2.3.

3. Results and discussion

3.1. Preliminary studies

Different colorimetric reactions for iron determination, namely with thiocyanate and bathophenanthroline (BPS), were tested to select the best reagent for the target concentration range. The results obtained in a batchwise approach, showed a significantly higher sensitivity (over 4-fold increase) for the reaction with BPS. The same comparison was performed on a paper approach using two layers of paper (Whatman 1 12.7 mm diameter) one layer with 12 μ L of reagent, as the top layer, and an empty bottom layer. The results also showed a significantly better sensitivity when using BPS, so it was the reagent chosen.

Because BPS reacts with Fe(II), a reducing agent was needed to convert Fe(III) in Fe(II) [22]. For the reduction, a 15 g/L hydroxylamine solution was chosen due to its proven efficiency in previous work [25]. Therefore, the reagent solution used in the development of the μ PAD for iron determination was a mixture of BPS and hydroxylamine (BPS_h). Different proportions of BPS and hydroxylamine were tested, based on what was reported by Marczenko [22], in order to attain a higher sensitivity with total conversion of Fe(III) in Fe(II). This was verified by comparing the calibration curves obtain from Fe(III) and Fe(II) standards, and as the calibration curves overlapped (relative deviation, RD < 2%), it confirmed that the Fe(III) was completely reduced to Fe(II).

3.2. Physical parameters – μ PAD assembly

First, the physical parameters of the μ PAD were studied, and a basic structure composed by two layers of paper discs was used. The idea was to force the sample/standard through a reagent layer and to have an empty layer below to promote the vertical flow and to serve as reservoir. The top layer, reagent layer, consisted in 9.5 mm diameter discs and the bottom layer consisted in 12.7 mm diameter Whatman 1 empty discs. The different paper discs sizes facilitated the alignment. To prepare the reagent layer, 12 μ L of the reagent, [BPS] = 100 g/L, was used and after 10 min oven dry (at 50^o C) aligned on top of the empty disc and laminated between the two sheets of the plastic pouches. This assembly enabled the insertion of 25 μ L of standard and time-to-scan (TTS) of 20

minutes. Filter papers with different paper treatments and porosities (see Electronic Supplementary Material, ESM Table 1) were tested on the reagent layer evaluating its influence in the calibration curve slope (Fig. 3).

Figure 3 here, please

3.2.1. Filter paper type

When different paper treatments were being compared, Whatman 1, 42, 50 and 541, the calibration curves obtained were very similar (Fig. 3a) except for the Whatman 50 paper, in which there was no full absorption of the standard and was excluded. As there were no significant differences in the sensitivities, Whatman 1 was chosen for being the paper without treatment (qualitative grade) and consequently being the most economic.

3.2.2. Filter paper porosity

Using the chosen qualitative type, the influence of the paper porosity (Whatman 1, 4 and 5), was studied and the highest sensitivity resulted from the paper Whatman 1, so it was the one chosen (Fig. 3b).

Due to the manual assembly process, and with a TTS of 20 min, it was observed that occasionally some units of the μ PAD card were not fully dry. To guarantee that the entire μ PAD was completely dry before scanning, a paper disk (Whatman 1) with diameter of 14 mm in the bottom (empty) layer was tested. Although there was no difference in the sensitivity (RD < 10%), the 14 mm discs did result in a more homogenous absorption in the entire μ PAD card, so it was chosen.

So, after the physical parameters study, a two-layer μ PAD with 9.5 mm and 14 mm Whatman 1 paper discs, for reagent and empty layer, respectively, was established.

3.3. Colorimetric reaction – iron determination

After establishing the physical assembly of the μ PAD, the influence of the BPS concentration was studied, to minimize consumption (batchwise studies were made a 100 g/L solution).

The conditions used in this study were 12 μL of the reagent with 10 min oven dry (at 50° C), 25 μL of standard and time-to-scan (TTS) of 20 minutes. To guarantee reagent excess, the lowest concentration of BPS to be studied was 0.5 g/L, corresponding to a BPS amount more than 5-fold the stoichiometric value of the highest iron standard. Consequently, for a 0.5 mg/L of iron standard, two BPS solutions with 0.5 g/L and 1 g/L were tested and the absorbance value increased 42% for the highest concentration. As a significant increase was observed, the BPS stock solution of 100 g/L was also tested, and the absorbance signal only increased 1%. This way, the BPS concentration of 1 g/L was set ensuring about a 10-fold excess over the stoichiometric value.

3.3.1. Reagent and sample/standard volume

The studies of both the reagent and the sample/standard volumes were made by establishing calibration curves for each tested volume and comparing the obtained slopes. Different reagent volumes, from 8 to 18 μL , were loaded in the reagent layer and, as the highest sensitivity was obtained with 10 μL of reagent, this was the chosen volume (Fig. 4a).

Figure 4 here, please

Then, sample volumes of 20, 25 and 30 μL were tested (Fig. 4b). Although there was an increase up to 25 μL , no significant difference was observed from 25 to 30 μL (RD < 10%). This could be a result of exceeding the reservoir capacity and so, if a higher sample volume had to be tested, the absorption capacity would have to be increased. The empty layer was initially composed of a Whatman 1 paper disk of 14 mm (section 3.2); to enhance the reservoir capacity, a Whatman 3 filter paper was tested. This filter paper is similar to Whatman 1, in respect to type and porosity (see Electronic Supplementary Material ESM Table1), but presents a higher thickness (0.39 mm over 0.18 mm). With Whatman 3 in the empty layer, 40 μL of sample/standard could be used (Fig. 4b) and a significant increase of the sensitivity (RD \approx 17%) was obtained, so 40 μL of sample was the volume chosen. Even though the μPAD card appeared to dry out in 15 min, the TTS was kept at 20 min to guarantee complete dryness.

3.4. Stability assessment

One of the main advantages of paper-based devices is the potential field application, so it is crucial to test both the storage stability of the μ PAD before use, and the stability of the colored product formed, after the sample/standard insertion.

3.4.1. Colored product stability

To evaluate the color product stability in the developed μ PAD, a calibration curve was prepared and the μ PADs scanned after the established TTS = 20 min. Then, a new scanning was made every 10 min for one hour and every hour up to 4 hours (see Electronic Supplementary Material ESM Fig. 1A). The calibration curve slopes obtained with the different scanning times were compared and no significant differences were observed up to 3 hours (RD = 9%) but after 4 hours after the sample insertion, a decrease in the sensitivity of 11% was observed. Therefore, the developed μ PAD presents a TTS window from 20 min up to 3 hours.

3.4.2. μ PAD stability

To test the stability of the μ PADs, several devices were prepared and stored in plastic bags (Lacor, 69053) at room temperature (approximately 21 °C) and protected from light. Two atmospheric conditions were used: air and vacuum, the latter obtained using a vacuum packaging machine (Henkovac – MINI/120-ST ECO).

Different periods were tested for each of the atmospheric conditions, ranging from 1 to 30 days (see Electronic Supplementary Material ESM Fig. 1B). At every studied period the stored μ PAD was used to perform a calibration curve and compared to calibration curve of a freshly assembled μ PAD prepared with the same set of standards.

A relative deviation below 10% was considered non-significant and the result showed that the devices were stable for a maximum of 15 days, in both atmospheric conditions.

3.5. Features of the developed μ PAD for iron determination

The main characteristics of the developed μ PAD are summarized in Table 1, including the dynamic range, the limit of detection, the limit of quantification and repeatability.

Table 1 Features of the developed μ PAD for iron determination; LOD, limit of detection; LOQ, limit of quantification; RSD, relative standard deviation;

Dynamic Range (mg/L)	Calibration Curve ^a $A = S \times [\text{Fe}] + b$	LOD ($\mu\text{g/L}$)	LOQ ($\mu\text{g/L}$)	Repeatability, RSD ^b	
				Intraday ^b	Interday ^c
0.065 – 1.2	$A = 2.05 \times 10^{-2}(\pm 9 \times 10^{-4}) \times [\text{Fe}] + 3 \times 10^{-4}(\pm 1 \times 10^{-4})$ $R^2=0.996\pm 0.003$	20	65	3%	6%

^a n = 3; ^b n = 5.

The limit of detection (LOD) and the limit of quantification (LOQ) were calculated according to IUPAC recommendations [26] as the concentration corresponding to three (LOD) and ten-times (LOQ) the standard deviation of the intercept (n = 3). The μ PAD repeatability was assessed by calculating the relative standard deviation (RSD) of five calibration curves in the same day, intraday RSD, and in consecutive days, interday RSD. The reagent consumption was calculated based upon the total volume of all reagent solutions used in the 20 discs of reagent layer of one μ PAD, and corresponded to 0.143 mg BPS, 0.857 mg hydroxylamine and 1.75mg HCl.

3.6. Interferences – urine matrix

Aiming for application to urine samples, the potential matrix interference was evaluated by comparing calibration curves slopes (sensitivity). Two sets of the developed μ PAD were assembled to perform a couple of calibration curves: one using iron standards prepared in water and one using iron standards prepared in synthetic urine (SU). The results showed a significant decrease in the calibration curve slope (Fig. 5a), indicating that at least one component of the synthetic urine is causing interference.

Based upon the synthetic urine composition, we narrowed down the potential source of the interference to three components: lactic acid (LA), citric acid (CA) or phosphate (P). In order to find which one cause interference, different solutions of synthetic urine were prepared, one without the three components (InSU_0) and then with each of the components added individually (InSU_LA, InSU_CA and InSU_P). These solutions were used to prepared iron standards and calibration curves performed (Fig. 5a).

Figure 5 here, please

It was possible to conclude that the other components in the synthetic urine (InSU_0) did not interfere as well as the lactic acid (InSU_LA), but that both the citric acid (InSU_CA) and the phosphate (InSU_P) caused a significant interference (Fig. 5a).

Then, to assess the maximum concentration possible to use without interference, calibration curves were established using iron standards prepared in synthetic urine with different concentrations of the citric acid (Fig. 5b) and phosphate (Fig. 5c). The maximum concentrations that did not display interference ($RD \leq 5\%$) were 0.26 mM for citric acid and 1.73 mM for phosphate.

3.7. Application to urine samples

3.7.1. Sample blank

Due to the urine potential intrinsic absorbance and the lack of a specific wavelength selection (detection based on RGB filter selection), some overlapping of the color product formed was expected. In fact, this would result in an increase in the measurement of pixels intensity and consequent absorbance calculation. To tackle this problem, a strategy was developed to include the measurement of a sample blank. The μ PAD assembly was adapted to include measurements without the color reagent, as described in section 2.2.1, to calculate the sample intrinsic absorbance. Then, that intrinsic absorption was subtracted from the calculated absorption obtained with the color reagent, according to the equation detailed also in section 2.2.1.

3.7.2. Validation

To assess the accuracy of the developed μ PAD for iron determination in urine samples, several samples (#26) were analyzed and the results compared to those obtained by AAS, atomic absorption spectrophotometry [24]. The relative deviation between the results obtained with the developed μ PAD ($[Fe]_{\mu PAD}$) and the AAS method ($[Fe]_{AAS}$) was calculated (see Electronic Supplementary Material ESM Table 2).

Figure 6 here, please.

A linear relationship between the two set of results (Fig. 6) was established: $[\text{Fe}]_{\text{AAS}} = 1.013 (\pm 0.039) \times [\text{Fe}]_{\mu\text{PAD}} + 0.002 (\pm 0.010)$, where the values in brackets correspond to the 95% confidence interval (of a t-student analysis). As the slope and the intercept were not statistically different from 1 and 0, respectively, there is no evidence for differences between the two sets of results and consequently the two methods.

Additionally, a t-test statistical analysis was made (see Electronic Supplementary Material ESM Table 3) and, for a 95% significance level, the obtained ρ -value was higher than the significance level ($\rho=0.882 > 0.05$) and the calculated t-value was 0.150 with a correspondent critical value of 2.01 (two-tail) indicating that the two sets of results are not statistically different.

So, the results obtained with the developed μPAD proved not only to be comparable to the atomic absorption results, but also that the working range was adequate for the analysis of the target samples.

4. Conclusions

In this work, a sensitive and portable microfluidic paper-based analytical device (μPAD) for iron determination in urine samples was developed. The device is capable of fast, on-hand measurements of iron in human urine samples without requiring pre-treatments. A range of 0.07 to 1.2 mg/L of iron, with a detection limit of 20 $\mu\text{g/L}$, proved suitable for all the analyzed samples (#26) and comparable to the determination by atomic absorption results ($\text{RD} < 9.5\%$).

The application of paper-based devices for iron determination in biological samples has been reported only once by Kamlesh Shrivastava (2020) [19] targeting water and blood plasma samples in a range of 50 to 900 $\mu\text{g/L}$ with limit of detection and quantification of 20 $\mu\text{g/L}$ and 65 $\mu\text{g/L}$, respectively. The described device in this work, attain identical limit of detection and quantification but was applied to a different biological sample, namely urine, handling with the intrinsic absorption of the sample.

The developed μPAD was envisioned to aid in health diagnosis, not only in healthcare facilities, but also in field application including remote areas. To meet the requirements

for that, stability studies were performed, and the developed μ PAD was stable for 15 days after assembling. After loading the sample, the device can be scanned within 3 hours, corresponding to the formed colored product stability. After usage, the μ PAD is disposable by incineration, which is not only environmentally friendly, but also an advantage when handling biological samples.

The main drawback of the developed device is its manual and laborious assembly, namely the delicate lamination process (avoiding the shifting of the discs), making it susceptible for an uneven distribution, potentially affecting reproducibility. However, this difficulty can be minimized if a mechanic aid could be used. The potential effect of this problem in the intensity readings is minimized by the elimination of the outliners. The developed μ PAD could ultimately be used as a screening option not only in healthcare facilities, but also as an aid in the diagnosis of some diseases and health conditions in the field application and remote locations.

Acknowledgments

F.T.S.M. Ferreira thanks FCT - Fundação para a Ciência e a Tecnologia for the grant SFRH/BD/144962/2019. This work was supported by National Funds from FCT - Fundação para a Ciência e a Tecnologia through project UIDB/50016/2020.

References

1. Linus Pauling Institute (2016) Iron | Linus Pauling Institute | Oregon State University. <https://lpi.oregonstate.edu/mic/minerals/iron>. Accessed 7 Sep 2020
2. Nakatani S, Nakatani A, Ishimura E, Toi N, Tsuda A, Mori K, Emoto M, Hirayama Y, Saito A, Inaba M (2018) Urinary Iron Excretion is Associated with Urinary Full-Length Megalin and Renal Oxidative Stress in Chronic Kidney Disease. *Kidney Blood Press Res* 43:458–470 . <https://doi.org/10.1159/000488470>
3. Marshfield Labs Iron, Urine (FEU). <https://www.marshfieldlabs.org/sites/ltrm/Human/Pages/22804.aspx>. Accessed 7 Sep 2020

4. Iron, Urine.
<http://www.labnet.health.nz/testmanager/index.php?fuseaction=main.DisplayTest&testid=284>. Accessed 17 Sep 2020
5. Iron, Urine - NMS Labs. <https://www.nmslabs.com/tests/2430U>. Accessed 17 Sep 2020
6. Petti CA, Polage CR, Quinn TC, Ronald AR, Sande MA (2006) Laboratory Medicine in Africa: A Barrier to Effective Health Care. *Clin Infect Dis* 42:377–382 . <https://doi.org/10.1086/499363>
7. McNerney R (2015) Diagnostics for Developing Countries. *Diagnostics* 5:200 . <https://doi.org/10.3390/DIAGNOSTICS5020200>
8. Almeida MIGS, Jayawardane BM, Kolev SD, McKelvie ID (2018) Developments of microfluidic paper-based analytical devices (μ PADs) for water analysis: A review. *Talanta* 177:176–190 . <https://doi.org/10.1016/J.TALANTA.2017.08.072>
9. Martinez AW, Phillips ST, Butte MJ, Whitesides GM (2007) Patterned Paper as a Platform for Inexpensive, Low-Volume, Portable Bioassays. *Angew Chemie* 119:1340–1342 . <https://doi.org/10.1002/ange.200603817>
10. Jiang X, Fan ZH (2016) Fabrication and Operation of Paper-Based Analytical Devices. *Annu Rev Anal Chem* 9:203–222 . <https://doi.org/10.1146/annurev-anchem-071015-041714>
11. Martinez AW, Phillips ST, Whitesides GM, Carrilho E (2010) Diagnostics for the developing world: Microfluidic paper-based analytical devices. *Anal Chem* 82:3–10 . <https://doi.org/10.1021/ac9013989>
12. Paper microfluidic devices : A review 2017 - Elveflow.
<https://www.elveflow.com/microfluidic-tutorials/microfluidic-reviews-and-tutorials/paper-microfluidic-devices-a-review-2017/>. Accessed 13 Dec 2018
13. Birch NC, Stickle DF (2003) Example of use of a desktop scanner for data acquisition in a colorimetric assay. *Clin Chim Acta* 333:95–96 . [https://doi.org/10.1016/S0009-8981\(03\)00168-2](https://doi.org/10.1016/S0009-8981(03)00168-2)
14. Ramdzan AN, Almeida MIGS, McCullough MJ, Kolev SD (2016) Development of a microfluidic paper-based analytical device for the determination of salivary aldehydes. *Anal Chim Acta* 919:47–54 . <https://doi.org/10.1016/j.aca.2016.03.030>

15. Yiannikourides A, Latunde-Dada G (2019) A Short Review of Iron Metabolism and Pathophysiology of Iron Disorders. *Medicines* 6:85 .
<https://doi.org/10.3390/medicines6030085>
16. Ems T, Huecker MR (2019) *Biochemistry, Iron Absorption*. StatPearls Publishing
17. Moniz T, Bassett CR, Almeida MIGS, Kolev SD, Rangel M, Mesquita RBR (2020) Use of an ether-derived 3-hydroxy-4-pyridinone chelator as a new chromogenic reagent in the development of a microfluidic paper-based analytical device for Fe(III) determination in natural waters. *Talanta* 214:120887 .
<https://doi.org/10.1016/j.talanta.2020.120887>
18. Ogawa K, Kaneta T (2016) Determination of iron ion in the water of a natural hot spring using microfluidic paper-based analytical devices. *Anal Sci* 32:31–34 .
<https://doi.org/10.2116/analsci.32.31>
19. Shrivastava K, Monisha, Kant T, Karbhal I, Kurrey R, Sahu B, Sinha D, Patra GK, Deb MK, Pervez S (2020) Smartphone coupled with paper-based chemical sensor for on-site determination of iron(III) in environmental and biological samples. *Anal Bioanal Chem* 412:1573–1583 . <https://doi.org/10.1007/s00216-019-02385-x>
20. Ferreira FTSM, Mesquita RBR, Rangel AOSS (2020) Novel microfluidic paper-based analytical devices (μ PADs) for the determination of nitrate and nitrite in human saliva. *Talanta* 219:121183 .
<https://doi.org/10.1016/j.talanta.2020.121183>
21. Hirayama T, Nagasawa H (2017) Chemical tools for detecting Fe ions. *J Clin Biochem Nutr* 60:39–48 . <https://doi.org/10.3164/jcbrn.16-70>
22. Marczenko Z, Balcerzak M (2000) *Separation, preconcentration, and spectrophotometry in inorganic analysis*, 1st ed. Elsevier Science
23. Machado A, Mesquita RBR, Oliveira S, Bordalo AA (2017) Development of a robust, fast screening method for the potentiometric determination of iodide in urine and salt samples. *Talanta* 167:688–694 .
<https://doi.org/10.1016/j.talanta.2017.03.017>
24. APHA, AWWA, WEF (1998) *Standard Methods for the Examination of Water and Wastewater*, 20th ed. Washington, DC
25. Santos IC, Mesquita RBR, Bordalo AA, Rangel AOSS (2015) Iodine speciation in coastal and inland bathing waters and seaweeds extracts using a sequential

injection standard addition flow-batch method. *Talanta* 133:7–14 .

<https://doi.org/10.1016/j.talanta.2014.01.025>

26. Currie LA (1995) Nomenclature in evaluation of analytical methods including detection and quantification capabilities (IUPAC Recommendations 1995). *Pure Appl Chem* 67:1699–1723 . <https://doi.org/10.1351/pac199567101699>

Figures

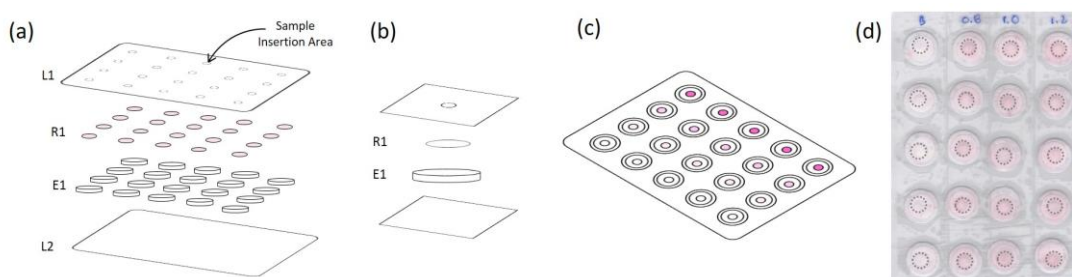


Fig. 1 Schematic representation of the μ PAD assembly for iron determination; a) indication of the layers alignments: L1, perforated top layer of the laminating pouch for sample/standard insertion; R1, reagent layer; E1, empty layer; L2, bottom layer of the laminating pouch; b) schematic representation of one unit of detection; c) schematic illustration of the top view of the μ PAD after standard placement; d) scanned image of the μ PAD (top view) with indication of the selected area for intensity measurement (dotted circles).

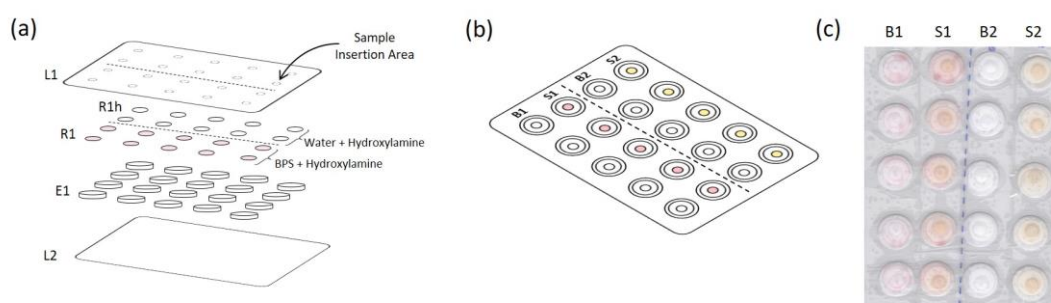


Fig. 2 Schematic representation of the sample μ PAD for iron determination in urine samples; a) layers assembly: L1, perforated top layer of the laminating pouch for sample/standard insertion; R1, BPS reagent (BPS + Hydroxylamine) layer; R1h, reagent without BPS (Water + Hydroxylamine) layer; E1, empty layer; L2, bottom layer of the laminating pouch; b) schematic representation (top view) of the placement of one urine sample with and without color reagent (S1 and S2) and the respective blanks (B1, blank of the color reaction and B2, blank of the urine color); c) scanned image of the μ PAD (top view).

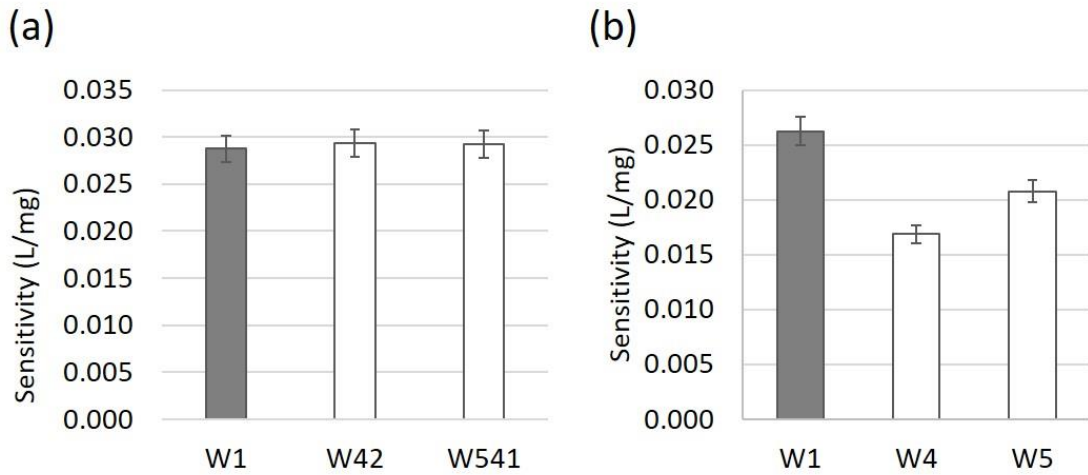


Fig. 3 Study of the influence in the calibration curve slope of different filter papers; a) papers with different treatments; b) qualitative filter papers with different porosities; the dark grey bars represent the chosen option; the error bars represent 5% deviation of the measurements.

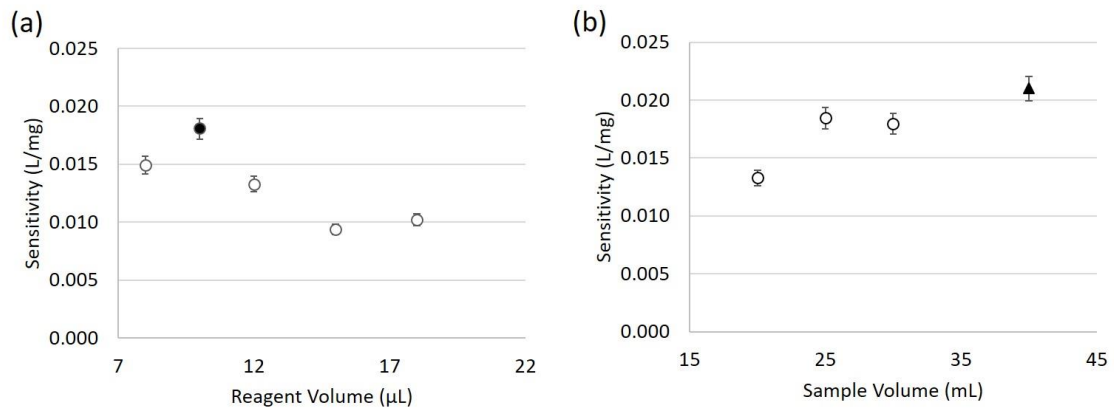


Fig. 4 Study of the influence in the calibration curve slope of the working volumes; a) the reagent volume; b) sample volumes where the circles represent µPADs with W1/W1 units and triangle represents µPADs with W1/W3 units; the points in black represent the chosen values; the error bars represent 5% standard deviation of the measurements.

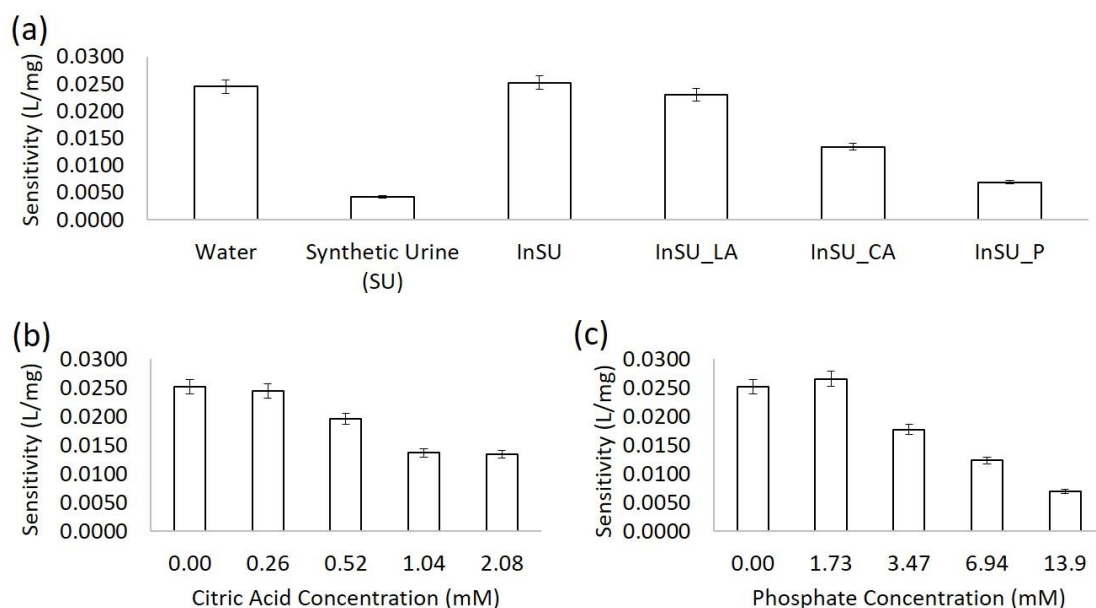


Fig. 5 Study of potential matrix interference on the calibration curve slope (sensitivity); a) iron standards prepared in: water, synthetic urine (SU), incomplete synthetic urine (InSU_0), incomplete synthetic urine with lactic acid (InSU_LA), incomplete synthetic urine with citric acid (InSU_CA) and incomplete synthetic urine with phosphate (InSU_P); b) iron standards prepared in synthetic urine with different concentration of citric acid; c) iron standards prepared in synthetic urine with different concentration of phosphate; the error bars represent 5% standard deviation of the measurements.

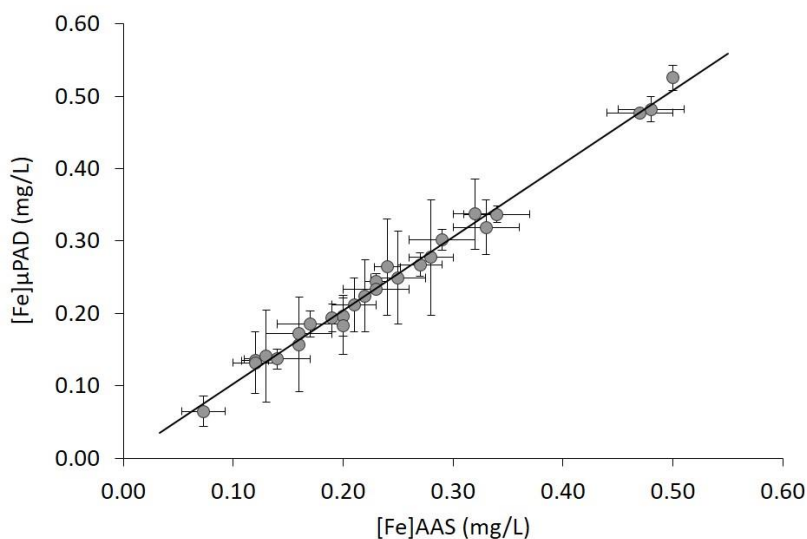


Fig. 6 Comparison between the results obtained for iron determination in urine samples (#26) with the developed μ PAD and the atomic absorption spectrometry (AAS); the error bars represent the standard deviation of the measurements and the full line represents the linear trendline between the two sets of results.